η^5-P- or η^4-P-Coordination in Apically Oxygenated Phosphoranes? An *Ab Initio* Study of PH_4O^-, $PH_4O^- \cdot E$ (E = Li^+, NH_4^+, and HF) and Related Fluorinated Oxyphosphoranes

Rainer Glaser* and Andrew Streitwieser[†]

Department of Chemistry, University of California, Berkeley, California 94720

Structural optimizations of the apically substituted isomer of PH_4O^- and the diapically substituted isomer of PH_3FO^- with diffuse-function augmented 3-21G* basis sets and with the 6-31+G* and 6-31++G* basis sets result in P-η^4-coordination in these anions. The structures obtained are those of a hydride or fluoride ion "solvated" by or complexed with phosphine oxide, rather than phosphoranes. In contrast, 3-21G* basis sets without diffuse functions on the atom in the *trans*-apical position with regard to the oxy-substituent yield P-η^5-phosphorane structures that appear to be computational artifacts of the small basis set; the formation of the P-η^4-geometries is curtailed by the insufficient functional description of the potential *trans*-apical nucleophilic leaving group. The overall neutral apical isomers of $PH_4O^- \cdot E(E = Li^+, NH_4^+)$, the diapical isomer of $PH_3FO^-Li^+$, as well as the model-solvated apical isomer of $PH_4O^- \cdot HF$ favor P-η^5-phosphorane geometries at all of these computational levels. The mechanism by which the E-group alters the electronic structures within $PH_4O_a^-$ is discussed based on the geometries, the molecular orbitals, and electron density analysis techniques.

INTRODUCTION

Although it is certainly desirable whenever possible to use large basis sets in molecular computations, the use of relatively small basis sets is still common, especially with large molecular systems. For many purposes small basis sets that incorporate at least split valence shells (such as 3-21G), and for some systems polarization functions (3-21G(*) or 3-21G*), give satisfactory geometries and relative energies. Thus, it is important to identify systematic limitations of such small basis sets. We present here an apparent such limitation and an approach that appears to minimize the limitation *while retaining the small basis set*.

In a previous theoretical study[1] from this group of monosubstituted model phosphoranes, PH_4X, relative energies, geometries, and electronic structures of a variety of apically and equatorially substituted phosphoranes were examined to study ligand apicophilicities. During these studies an unusually long *trans*-apical PH-bond was found for the apically substituted phos-

phoranyl anion PH_4O^- that indicated a tendency toward dissociation of such oxygenated phosphoranes into a hydride closely associated with a phosphine oxide molecule. In this article we present a more detailed study of the anions PH_4O^- and PH_3FO^- with focus on their apically or diapically substituted isomers, respectively. Calculations with diffuse-function augmented 3-21G* and 6-31G* basis sets indicate that the P-η^5-phosphorane structures of the apically substituted oxyphosphoranyl anions are artifacts. The dissociation of the phosphoranyl anion to an H_3PO-conplexed hydride (fluoride) is prevented by an absence of diffuse functions in the AO-basis of the *trans*-apical hydrogen (fluorine). The artificial P-η^5-phosphorane structures of the anions may be regarded as the result of a basis set superposition problem;[2] that is, the *trans*-apical leaving group uses basis functions centered on the atoms of the remainder of the molecule to partially compensate for the inability of its AO-bases to sufficiently describe the electron density of this nucleophilic group. With small basis sets the electrons tend to go where the functions are and it is important to know the limitations of using relatively small basis sets. Thus, these anions are compared to their derivatives $PH_4O^- \cdot E$ with E = Li^+, NH_4^+, or HF and of $PH_3FO^-Li^+$. In the neutral derivatives complete dissociation of

---

the *trans*-apical PH- or PF-bonds seems unlikely since a "solvent" (PH_3O) separated ion pair would be formed, but a tendency toward P-η^4-coordinated structures similar to the one observed in the anions might be anticipated.

COMPUTATIONAL ASPECTS

Standard single-determinant restricted Hartree–Fock calculations were performed with the programs[3] Gaussian 82 and Gaussian 90. Gradient optimizations[4] were carried out under the constraints of the symmetry point group specified unless otherwise noted. Supplemented versions of the basis sets 3-21G(*) and 6-31G* were used. The standard 3-21G(*) basis set[5] was slightly modified in that sets of six *d*-type functions were added to all first-row elements except lithium. These *d*-type functions serve primarily to improve the unsaturated *s,p*-AO-bases (as opposed to true *d*-orbital participation) and they are essential for that purpose.[1,6] The exponents of these polarization functions were taken from the 6-31G* basis set[7] and the resulting basis set is denoted 3-21G*. In the present study the recently recommended[5] *d*-exponent of 0.55 is used for phosphorus. Earlier calculations[1] made use of the preliminary P-*d*-exponent of 0.47; the use of this *d*-exponent is indicated by a prime in the basis set notation(3-21G*'). The effects of the different phosphorus *d*-exponent on structures and relative energies are small.[8] The anionic oxyphosphoranes PH_4O^-, PH_3FO^-, and their derivatives $PH_4O^- \cdot E$ and $PH_3FO^- \cdot E$ (E = Li^+, HF, NH_4^+) were calculated with the implementation of a shell of diffuse *s*- and *p*-functions on oxygen (3-21+(O)G*) to allow for a better description of the O-lone pairs. In several calculations a diffuse *sp*-shell or a single flat *s*-function was added to fluorine or hydrogen, respectively, with the exponents recommended by Schleyer et al.[9] The augmentation of the AO-basis of a hydrogen or a fluorine atom by (one) diffuse function(s) is indicated in the basis set notation as follows: 3-21+(H_a)G* indicates, for example, that a diffuse *s*-function was added to the *trans*-apical hydrogen atom. Calculations with the standard basis sets[7,9] 6-31+G* and 6-31++G* were carried out to judge the quality of the results obtained with these supplemented 3-21G(*) basis sets.

Projection electron density functions, P(x, z), and cross-sections of the electron density were determined from the 3-21G* wave functions with the program PROJ.[10] Demarkation of spatial regions[11] of P(x, z) and numerical integrations of the contained projected electron density yield integrated projection populations (IPP).[12] The IPP-values approximate atomic populations obtained by Bader's method of integration over atomic *basins* demarked by the zero-flux surface of the 3-D electron density distribution.[13] The approximation of such surfaces by vertical-curtain-type surfaces has been analyzed recently;[14] the use of the IPP method in the present study is sufficiently valid and is justified by the great gain in computational speed.

RESULTS AND DISCUSSION

Geometries of the Anions PH_4O^- and PH_3FO^-

Computed structures of PH_4O^- are listed in Table I. Optimization of the apically oxygenated C_{3v}-symmetric anion PH_4O^- at RHF/3-21+(O)G* resulted in a phosphorane structure with an exceptionally long apical PH-bond of 1.589 Å (1.584 Å at 3-21+(O)G*', Reference 2) indicative of the tendency of this anion toward dissociation of phosphine oxide and hydride ion. Supplementation of this basis set with an additional diffuse *s*-function to the *trans*-apical hydrogen, 3-21+(H_a, O)G*, gave a P-η^4-coordinated structure with an apical PH-bond of 2.932 Å and a shorter PO-bond of 1.496 Å. The resulting structure is essentially that of a hydride ion closely associated with phosphine oxide, $H^- \cdot H_3PO$. The PO-bond length is only 0.04 Å longer and the OPH_e-angle (114.7°) is only 3.1° less than in PH_3O.[15,16a] Similar complexes are obtained at the levels RHF/6-31+G* and RHF/6-31++G*. With the 6-31+G* basis sets a P-η^4-coordinated structure resulted even without diffuse functions on the *trans*-apical hydrogen atom, but the apical PH-bond length increases significantly in going to the 6-31++G* level. As expected, the *trans*-apical PH-bond found at RHF/3-21+(H_a, O)G* is longer (by 0.1 Å) compared to the bond length determined with the more balanced basis set 6-31++G*. At both of the levels 6-31+G* and 6-31++G* the PH_3O-geometry differs but marginally from that of isolated phosphine oxide.[16b]

These results suggest that the preferred apically substituted structure of PH_4O^- is a PH_3O complexed hydride ion rather than a P-η^5-coordinated phosphorane. Phosphorane geometries of the apical substituted PH_4O^- are artifacts caused by basis set inadequacies. The earlier 4-31G calculations of Deakyne and Allen[17] showing axial addition of hydride ion to phosphine oxide apparently manifest these same artifacts.

Similar basis set effects are also found for oxygenated fluorophosphoranyl anions such as PH_3FO^- (Table II). For $PH_3F_aO_a^-$, a phosphorane structure with a longer than usual *trans*-apical PF-bond of 1.709 Å was obtained at 3-21+(O)G*.

Table I. Geometries of PH_4O^- and $PH_4O^- \cdot E$ ($E = Li^+, HF, NH_4^+$).[a]

Parameter	3-21+(O)G*		3-21+(H$_a$,O)G*	6-31+G*		6-31++G*
	C$_{2v}$	C$_{3v}$	C$_{3v}$	C$_{2v}$	C$_{3v}$	C$_{3v}$
PH$_4$O$^-$						
PH$_a$	1.484	1.589	2.932	1.493	2.560	2.831
PH$_e$	1.434	1.414	1.383	1.432	1.384	1.385
PO	1.531	1.547	1.496	1.518	1.497	1.490
H$_e$PO	128.538	99.183	114.676	129.004	113.583	114.605
H$_a$PO	94.406			93.618		
PH$_4$O$^-$Li$^+$						
PH$_a$	1.456	1.482	1.491	1.456	1.488	1.489
PH$_e$	1.413	1.403	1.401	1.413	1.403	1.403
PO	1.576	1.618	1.617	1.571	1.613	1.613
H$_e$PO	127.770	94.024	94.198	127.776	98.083	94.103
H$_a$PO	90.283			89.954		
LiO	1.634	1.626	1.625	1.636	1.627	1.627
PH$_4$O$^-$ · HF						
PH$_a$		1.557	1.627		1.578	* 1.599
PH$_e$		1.410	1.400		1.409	1.406
PO		1.558	1.553		1.551	1.549
H$_e$PO		97.928	99.063		98.043	98.441
OH		1.519	1.523		1.493	1.498
HF		0.957	0.956		0.974	0.972
PH$_4$O$^-$ · NH$_4^+$						
PH$_a$		1.493	1.501		1.499	1.503
PH$_e$		1.404	1.402		1.406	1.405
PO		1.605	1.604		1.598	1.597
H$_e$PO		94.838	94.979		94.916	94.972
OH		1.393	1.394		1.379	1.380
NH[b]		1.023	1.023		1.029	1.029

[a]In Å and degrees.
[b]Not optimized, value as in NH_4^+ optimized at 3-21G* (T_d).

Table II. Geometries of isomeric structures of $PH_3F_aO^-$ and $PH_3F_aO^-Li^+$.[a]

Parameter	3-21+(O)G*		3-21+(H$_a$,O)G*	6-31+G*	
	C$_s$	C$_{3v}$	C$_{3v}$	C$_s$	C$_{3v}$
PH$_3$F$_a$O$^-$					
PH$_a$	1.482			1.472	
PH$_e$	1.416	1.408	1.379	1.400	1.381
PO	1.515	1.551	1.508	1.497	1.501
PF	1.648	1.709	2.427	1.804	2.434
H$_e$PF	86.337	82.532	68.826	81.893	68.529
H$_a$PO	97.446			99.798	
FPO	96.117			96.054	
H$_e$PFO	123.511			122.972	
PH$_3$F$_a$O$^-$Li$^+$					
PH$_a$	1.449			1.442	
PH$_e$	1.398	1.391	1.382	1.390	1.383
PO	1.556	1.616	1.599	1.540	1.594
PF	1.627	1.639	1.756	1.725	1.772
H$_e$PF	88.292	87.072	83.403	85.001	83.023
H$_a$PO	93.412			95.361	
FPO	92.161			91.874	
H$_e$PFO	122.387			121.835	
LiO	1.630	1.621	1.631	1.640	1.632

[a]In Å and degrees.

Supplementation of the F-AO-basis by an additional diffuse sp-shell suffices to effect a change from P-η^5- to P-η^4-coordination; the PF$_a$-bond lengthened to 2.427 Å and the PO-bond length decreased by 0.043 Å to 1.508 Å. This geometry is in close agreement with that computed at RHF/6-31+G*. The diapically substituted structure of PH_3FO^- is best described as a fluoride ion

complexed with phosphine oxide, $F^- \cdot H_3PO$, rather than as a phosphorane.

Structures, Energies, and Apicophilicities of Derivatives of PH_4O^- and PH_3FO^-

For our studies of the electronic structures of multiply substituted phosphoranes it was important to include phosphoranes that contain a PO-bond with an essentially *anionic oxygen* [18] for comparative purposes.[19] Since systems of the type PH_4O^- and PH_3FO^- cannot be used for this purpose (*vide supra*) it appeared promising to study derivatives of the type $PH_4O^- \cdot E$ in which the oxy-substituent remains highly charged but no longer affects dissociation to a P-η^4-coordinated species.

Optimized geometries of the systems $PH_4O^- \cdot E$ ($E = Li^+$, HF, NH_4^+) are listed in Table I and the geometries of the lithium derivatives of PH_3FO^- are given in Table II. Energies are summarized in Table III.

Aside from the constraints imposed by the C_{3v}-symmetry the model system $PH_4O^- \cdot NH_4^+$ was constrained further. The NH-bond length of NH_4^+ optimal at 3-21G* (1.023 Å) was used in the system $PH_4O^- \cdot NH_4^+$. Furthermore, the ammonium ion was oriented in such a way as to point one of the NH-bonds directly at the phosphorane oxygen atom. This orientation was chosen (instead of a more stable arrangement involving three hydrogen bonds) to keep the positive center farther away from the O^--substituent. Also, the POLi-angle was fixed to 180.0° in the optimization of the C_s-symmetric structure of $PH_3FO^-Li^+$.

The lithio derivatives both of the apically and of the equatorially substituted (fluorinated) oxyphosphoranyl anions were optimized with the basis sets 3-21+(O)G* and 6-31+G*. In addition, geometries were optimized with the 3-21+(H_aF_a,O)G* and the 6-31++G* basis sets for those structures that contain the oxy-substituent

in the apical position to allow for a more flexible AO-description of the atom that is positioned *trans*-apical with regard to the oxy-substituent. For the model systems $PH_4O^- \cdot E$ with $E = HF$ or NH_4^+ the C_{3v}-symmetric structures were examined with all four basis sets.

Derivatives of Oxophosphoranyloxy Anion

Bond lengths in the narrow range of 1.82–1.89 Å resulted for the *trans*-apical PH-bond in the apically substituted molecule $PH_4O^-Li^+$. In contrast to the free anion $PH_4O_a^-$ the lithio-derivative clearly prefers the P-η^5-coordinated phosphorane structure and shows no tendency toward dissociation of the *trans*-apical PH-bond; these PH_a-bond lengths are typical for phosphoranes.[1] The equatorial PH-bonds (1.403 ê) shorten marginally upon ion pair formation, the PO-bond increases by about 0.120 Å, and the H_ePO-angle is reduced from about 114° in PH_4O^- to about 94° in $PH_4O^-Li^+$ (Table I). Whereas the 3-21+(O)G* structure of the free anion greatly (and artificially) differed from those obtained with the other basis sets, all of the geometries of its lithio-derivative are virtually the same.

The structural differences between $PH_4O_a^-$ and $PH_4O_a^-Li^+$ suggest that the Li^+ polarizes and localizes the electron density at oxygen and that the π-donating capability of the oxygen is thus reduced. The characteristics of the molecular orbitals support this conclusion. The valence MOs of the C_{3v}-symmetric isomer of $PH_4O^-Li^+$ ($6a_1$, $7a_1$, $2e$, $8a_1$, $3e$, and $9a_1$) correspond in their gross features to the valence MOs ($5a_1$, $6a_1$, $2e$, $7a_1$, $3e$, and $8a_1$) of PH_4O^-; contour plots of these MOs of the anion have been given previously.[1] Accordingly, the $6a_1$ and $7a_1$ orbitals are formed by symmetric and antisymmetric combinations, respectively, of s-type functions on phosphorus and oxygen. The orbitals $8a_1$ and $9a_1$ are formed mainly by the symmetric and antisymmetric combinations of sp_z-hybridized atomic orbitals on

Table III. Total energies[a] of PH_4O^-, PH_3FO^-, and their derivatives $PH_4O^- \cdot E$ ($E = Li^+$, HF, NH_4^+) and $PH_3FO^-Li^+$.[a]

Molecule		3-21+(O)G*	3-21+(H/F,O)G*	6-31+G*	6-31++G*
PH_4O^-	C_{3v}	415.813423	415.838976	417.819361	417.829413
	C_{2v}	415.829322		417.822255	
$PH_4O^-Li^+$	C_{3v}	423.280946	423.281811	425.319342	425.319543
	C_{2v}	423.283666		425.319868	
$PH_4O^- \cdot HF$	C_{3v}	515.359957	515.361884	517.873169	517.874692
$PH_4O^- \cdot NH_4^+$	C_{3v}	472.290131	472.290755	474.547397	474.548334
PH_3FO^-	C_{3v}	514.256047		516.777544	
	C_s	514.279128		516.773596	
$PH_3FO^-Li^+$	C_{3v}	521.721331	521.766830	524.259779	
	C_s	521.730436		524.260133	

[a] −E in atomic units.

phosphorus and oxygen. The oxygen substituent interacts with the π-system through two sets of degenerate orbitals, $2e$ and $3e$, which involve bonding and antibonding, respectively, to the equatorial hydrogens. Localization of electron density at oxygen should cause MOs that are PO-bonding to become destabilized while those MOs with PO-antibonding character should become stabilized. The eigenvalues of the valence MOs[20] of PH$_4$O$^-$Li$^+$ show that the $2e$-MOs are destabilized significantly compared to PH$_4$O$^-$; the increased PO-bond length in the lithium compound provides further support for this argument. On the other hand, the reduced π-donating capability decreases the antibonding character between the equatorial hydrogens and the oxygen in the $3e$-orbitals and the OPH$_e$-angle decreases. The most significant difference between PH$_4$O$^-$ and the neutral molecule PH$_4$O$^-$Li$^+$ is the extreme decrease of the *trans*-apical PH-bond length. The bonding between phosphorus and the apical hydrogen is largely associated with the σ-orbitals $8a_1$ and $9a_1$ (HOMO). The HOMO PH$_4$O$^-$Li$^+$ corresponds essentially to the HOMO of PH$_4$O$^-$ but they differ in the amount of p_z-character; as expected, the p_z-character in the HOMO of PH$_4$O$^-$Li$^+$ is larger than in the $8a_1$-orbital of PH$_4$O$^-$. The σ-lone pair of oxygen becomes more stabilized the better it is directed toward the lithium cation, that is, the larger the p_z-character is at oxygen in the HOMO. Simultaneously, the contributions of the p_z-type atomic orbitals of phosphorus to the HOMO are increased and the bonding of phosphorus with the *trans*-apical hydrogen is enhanced; the PH$_a$-bond length decreases.

In the equatorially O$^-$-substituted phosphorane the same trends are observed when Li$^+$ is associated with PH$_4$O$_e^-$ (Table I). The effects are less significant compared to the apically substituted cases and it is for this reason that only the apically substituted isomers of PH$_4$O$^-$ · E (E = HF, NH$_4^+$) are considered in this work.

The apicophilicities calculated for the O$^-$-substituent are 10.0 and 9.3 kcal/mol at 3-21+(O)G* and 3-21+(O)G*', respectively. With the larger basis sets no apically substituted phosphorane structure exists on the respective potential energy surfaces of PH$_4$O$^-$ and apicophilicity becomes undefined. At RHF/6-31+G* the C$_{2v}$-symmetric phosphorane is 1.82 kcal/mol more stable than the C$_{3v}$-symmetric H$^-$ · H$_3$PO-structure. For the lithio-derivatives small site-preference energies of 1.7 and 0.33 kcal/mol, respectively, are found at 3-21+(O)G* and at RHF/6-31+G*; that is, the O$^-$-substituent exhibits a small preference for the equatorial position under chemical conditions in which a closely associated cation is present.

The complexation of the apically substituted isomer of PH$_4$O$^-$ with hydrogen fluoride results in smaller but similar structural effects compared to PH$_4$O$^-$Li$^+$. The structures indicate little basis set dependence except for the H-bonding distance (which is somewhat larger with the 3-21G* basis sets than with the 6-31G* basis sets) and for the overestimated PH$_a$-bond length in the 3-21+(H$_a$, O)G* structure (probably caused by basis set unbalance). This result suggests that the involvement of the oxo-substituent in H-bonding is sufficient to prevent the dissociation to a P-η^4-coordinated structure.

In PH$_4$O$^-$ · HNH$_3^+$ H-bonding and overall neutrality of the molecule are combined. This model system behaves virtually identically to the lithium derivative. As with the lithio-derivatives basis set effects on structures are minimal.

Derivatives of Fluorinated Oxophosphoranyloxy Anion

The structural changes upon association of PH$_3$FO$^-$ with Li$^+$ follow the same pattern as with the lithium derivative of PH$_4$O$^-$: the PO-bond lengths are increased while the PF- and the PH-bond lengths are shortened concomitantly. As expected, the diffuse-function augmented basis sets 3-21+(F, O)G* and 6-31+G* yield significantly longer PF-bonds, moderately shorter PO-bonds, and decreased H$_e$PF-angles compared to the 3-21+(O)F* structure (Table II), but the structures of the lithio-derivatives clearly remain phosphorane structures.

Basis set effects on site-preference energies are large. Whereas the structure of PH$_3$F$_a$O$_e^-$ is preferred by 14.5 kcal/mol over the di-apical structure at RHF/3-21+(O)G*, the energy difference is reduced to 5.7 kcal/mol for the overall neutral lithium compounds. With the RHF/6-31+G* energies the C$_{3v}$-symmetric anion is preferred by 2.5 kcal/mol, but in the case of the lithio-derivatives the C$_s$-symmetric structure is favored 0.2 kcal/mol. This change in the relative isomer stability apparently reflects the reduced preference of the LiO-substituent for the equatorial position, but it remains to be seen just how meaningful are site-preference energies determined at RHF/6-31+G*.

Electron Density Analysis

In applying the techniques of electron density analysis we can adopt two philosophies. Most frequently, the electron density distributions of stationary structures are analyzed and their topological properties as well as the derived properties, such as integrated populations, are compared. In an alternative approach, the elec-

tron densities of only partially optimized structures are compared and these comparisons are especially useful since they are amenable to graphical representation in the form of electron density difference diagrams. The latter approach yields valuable insights into the electronic reasons that *cause* geometrical relaxation, while the other approach quantitatively describes the *consequences* of such geometrical and electronic relaxation. In the present study both of these approaches have been applied. First, contour diagrams of electron density difference cross-sections are analysed with focus on the substituent effects on the PH-bonding regions. Subsequently, the projection electron density functions are discussed as determined for the optimized structures.

Cross-sections of the valence electron density and projection electron density functions were determined for the molecules PH_4O^- and $PH_4O^- \cdot E$ ($E = Li^+, HF, NH_4^+$). For our purposes the analysis of electron density difference cross-sections requires the use of partially optimized structures in which the PH_4-fragments are alike. The PH-bond lengths calculated for PH_5 at 3-21G*' ($PH_a = 1.473$ Å and $PH_e = 1.411$ Å) were used in the PH_4-fragments in all of the standard optimized structures.[21] The differences between the fully and the partially optimized structures of the systems $PH_4O^- \cdot E$ as well as the relative energies of corresponding sets of structures are comparatively small.[8,21] The electron density analysis based on these standard structures should thus not only provide insights into the electronic driving forces that lead to geometry relaxation, but may also be regarded as a first approximation to the differences in the electronic structures of the fully optimized structures. The latter, however, is certainly not true for the parent system PH_4O^- itself. The requirement of an ideal trigonal-pyramidal P-environment in the partially optimized structures will force a phosphorane structure for $PH_4O_a^-$ with any reasonable basis set and the use of the 3-21G* wave function for PH_4O^- therefore appears justified in the analysis of the standard structures. But in the discussion of the projection functions the data for the (artificial) structure of PH_4O^- merely serve to compare the electronic structure of the hypothetical anionic phosphorane to the true phosphorane structures of the derivatives $PH_4O^- \cdot E$.

Cross-Sections of (Difference) Electron Density Distributions

Figures 1 and 2 show cross-sections of the 3-21G* electron density distributions[22] of PH_4O^- and $PH_3O^-Li^+$, respectively, and of their relative

electron densities with regard to PH_5. The reduced π-donation from oxygen to the PH_4-fragment in the neutral compound is clearly evident. Both PH_4O^- and its lithium derivative have excess electron density at the equatorial hydrogens compared to PH_5, but this excess is much smaller for the neutral compound. The difference plots thus reveal the electronic reason for the different H_ePO-angles and PH_e-bond lengths in the anionic and the neutral compounds. While the inductive interactions through the $8a_1$ — and the $9a_1$ — orbitals are not easily discernable by examination of the molecular orbitals, the effects of these interactions are manifest unambiguously in the electron density difference maps. The lithium cation causes *less* depletion of electron density in the bonding region of the *trans*-apical PH-bond of $PH_4O^-Li^+$ compared to PH_4O^-. This finding explains why the lithioderivative shows no tendency toward dissociation of the *trans*-apical PH-bond. Similar calculations with a point positive charge instead of Li^+ and with the geometry of $PH_4O^-Li^+$ result in the cross-sections shown in Figure 3. The depletion of electron density along the PO-bond is slightly more pronounced in the case of the point charge, but the effects of a lithium cation and a single positive point charge are virtually identical and this similarity emphasizes the largely ionic character of the LiO bond in $PH_4O^-Li^+$. The changes in the electron distribution in the PH_4-fragment upon association of PH_4O^- with Li^+ can be further examined with electron density differences cross-sections obtained by subtraction of the cross-sections of $PH_4O^-Li^+$ and PH_4O^- from each other, $\rho(PH_4O^-Li^+) - \rho(PH_4O^-)$. Figure 4 shows Li^+ to cause a shift of electron density from the hydrogens into the PH-bonding regions and, moreover, this plot reveals the polarization of the electron density of the O^--substituent by Li^+ that localizes electron density at oxygen and reduces the π-donating capability of the substituent.

The electronic effects of an H-bonding solvent molecule were studied with the model system $PH_4O^- \cdot HF$ (Fig. 5). The difference cross-section $\rho(PH_4O^- \cdot HF) - \rho(PH_5)$ closely resembles the corresponding plot for the anionic molecule, $\rho(PH_4O^-) - \rho(PH_5)$. Despite the H-bonding a large excess of electron density persists on the hydrogens of the PH_4-fragment and the electron density along the PH-bonds remains significantly depleted. We noted above that the *trans*-apical PH-bond in the this system is longer than in the overall neutral systems (Table I) but that $PH_4O^- \cdot HF$, unlike PH_4O^-, remains a phosphorane. The analysis of the projection electron density functions helps to further clarify the effects of HF on the PH_4O^- (*vide infra*).

The contour maps of the electron density cross-sections of the system $PH_4O^- \cdot NH_4^+$ are shown
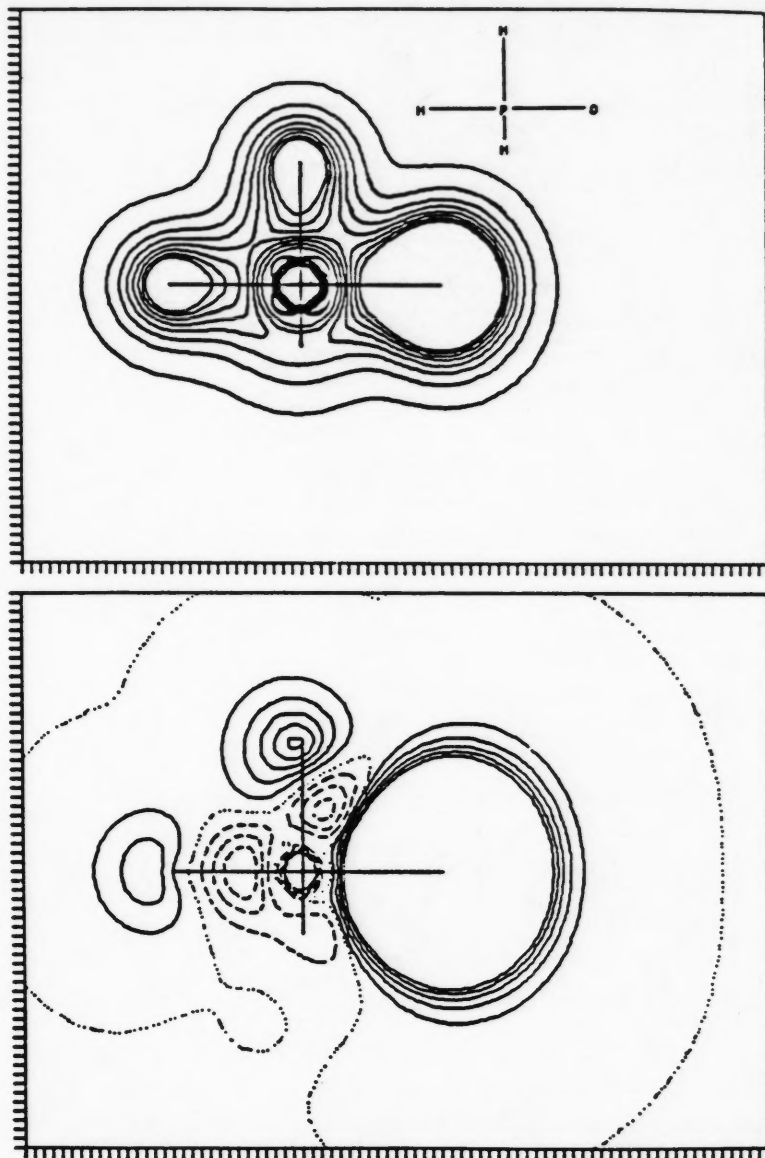
Figure 1. On top the contour diagram is shown of the 3-21G* valence electron density cross-section of PH$_4$O$^-$ (C$_{3v}$) with levels from 0.01 to 0.15 by 0.02 e a.u.$^{-3}$ The plot at the bottom shows the difference of the electron density cross-sections between PH$_4$O$^-$ and PH$_5$, ρ(PH$_4$O$^-$) $-$ ρ(PH$_5$), with contour levels from -0.01 to 0.01 by 0.002 e a.u.$^{-3}$.

in Figure 6. The similarity of these plots and the respective plots calculated for the lithium species suggests that the major requirement for localization of the charge on the PH$_4$O$^-$-fragment is overall neutrality of the system.

Projected Electron Density Functions

The projection functions of the total electron densities were calculated for the C$_{2v}$- and C$_{3v}$-symmetric isomers of PH$_4$O$^-$ and PH$_4$O$^-$Li$^+$, for the C$_{3v}$-symmetric systems PH$_4$O$^-$ · E (E = HF, NH$_4$$^+$), and for the parent molecule PH$_5$. The contour maps obtained for PH$_4$O$^-$ and PH$_4$O$^-$Li$^+$ are shown in Figures 7 and 8 (top: C$_{3v}$; bottom: C$_{2v}$), respectively, and the projection functions calculated for the molecules PH$_4$O$^-$ · E (E = HF, NH$_4$$^+$) are shown in Figure 9. The contour levels are from 0.005 to 0.605 by 0.05 e a.u.$^{-2}$ in all cases. Integrations of the electron densities in the demarked (dotted lines) regions yield the IP-P-values which are listed in Table IV together
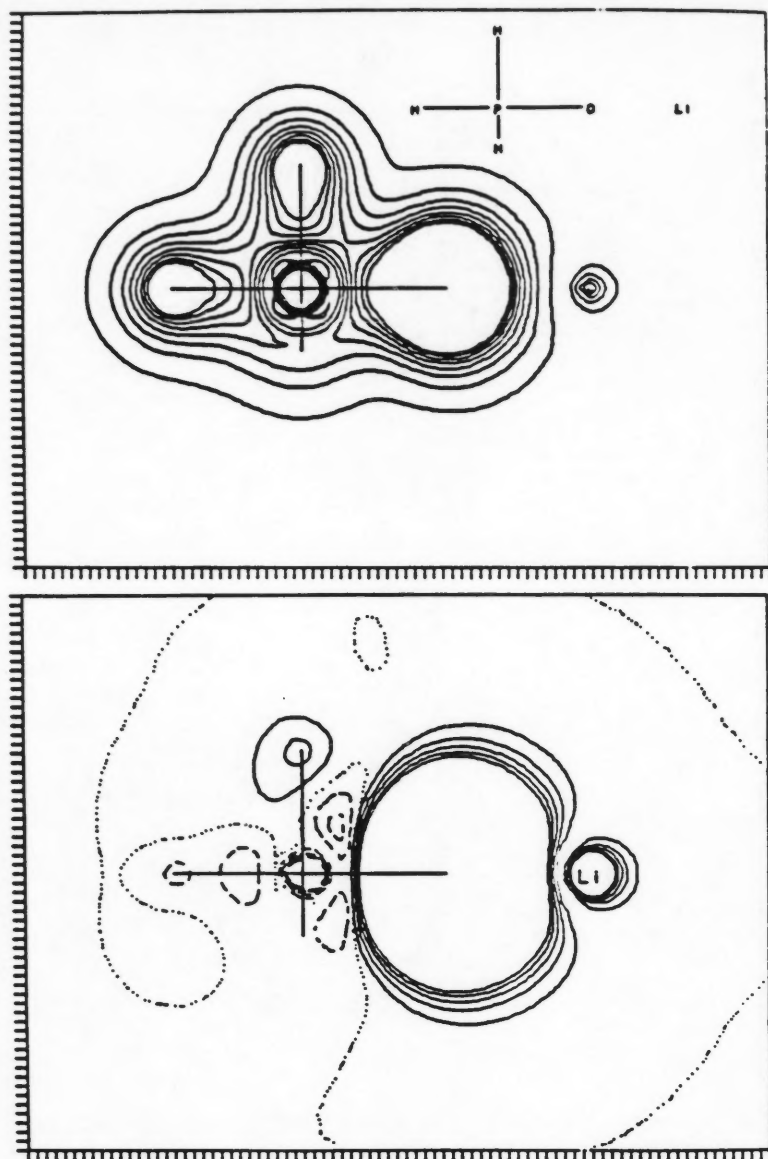
Figure 2. On top the contour diagram is shown of the 3-21G* valence electron density cross-section of the $PH_4O^-Li^+$ (C_{3v}). The plot at the bottom shows the difference of the electron density cross-sections between $PH_4O^-Li^+$ and PH_5, $\rho(PH_4O^-Li^+) - \rho(PH_5)$. Contour levels are as in Figure 1.

with the minimum values of the projected electron density (MPD in e a.u.$^{-2}$) along the respective bonds. These data allow for a more quantitative discussion of the electron density shifts found in the electron density cross-sections.

The MPD-values of the apical and the equatorial PH-bonds in PH_5 are 0.37 and 0.38 e a.u.$^{-2}$, respectively. In the anion PH_4O^- the MPD-values are decreased in agreement with the depletion of electron density along the PH-bonds found in the cross-sections. The decrease is more pronounced for the apical (MPD = 0.32 e a.u.$^{-2}$)

than for the equatorial PH-bond (MPD = 0.37 e a.u.$^{-2}$) in $PH_4O_a^-$. For the C_{2v}-symmetric anion $PH_4O_e^-$ a decrease of the MPD-value of the apical PH-bond to 0.35 e a.u.$^{-2}$ is found as well. On the other hand, the respective values for the neutral system $PH_4O^- \cdot E$ ($E = Li^+, NH_4^+$) are less than 0.01 e a.u.$^{-2}$ smaller than the values for PH_5. The MPD-values show, in agreement with the cross-sections, that the cation causes an increase of electron density in the PH-bonding regions compared to PH_4O^-. The model-system $PH_4O^- \cdot HF$ behaves differently;
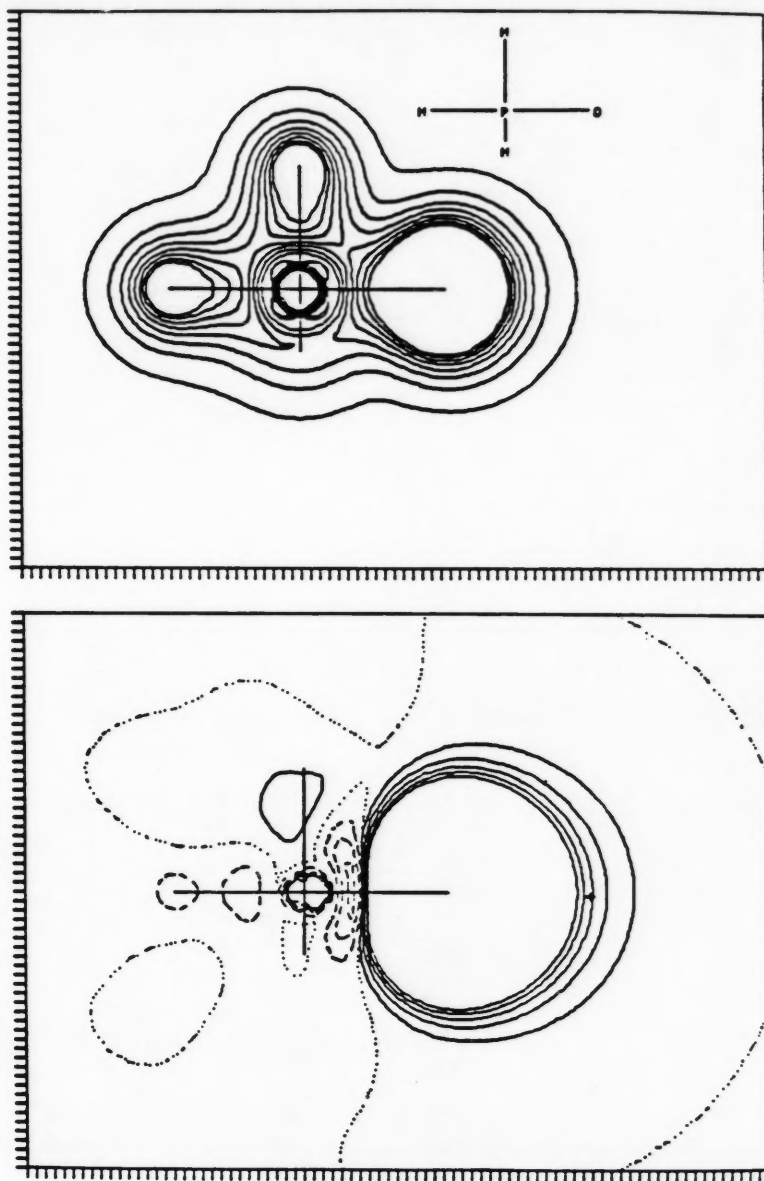
Figure 3. On top the contour diagram is shown of the 3-21G* valence electron density cross-section of PH$_4$O$^-$ (C$_{3v}$) under the influence of a point positive charge (PPC). The geometry of PH$_4$O$^-$ in the standard optimized structure of PH$_4$O$^-$Li$^+$ is used and Li$^+$ is replaced by the point charge. At the bottom the difference plot is shown that results from subtraction of the cross-sections of PH$_4$O$^-$ · PPC and PH$_5$, ρ(PH$_4$O$^-$ · PPC) − ρ(PH$_5$). Contour levels are as in Figure 1.

in this case the MPD-value of the apical bond is 0.33 e a.u.$^{-2}$ and closer to the corresponding value of PH$_4$O$^-$ than of PH$_5$ whereas the MPD-value of the equatorial PH-bond is essentially that determined for PH$_5$.

The IPP-values for the apical and the equatorial hydrogens in PH$_5$ are 1.27 and 1.18 electrons, respectively.[23] These values are greatly increased in both isomers of PH$_4$O$^-$

where quite similar charges of −0.45 and −0.44 were found for the apical and the equatorial hydrogens, respectively.[25] The presence of Li$^+$ or NH$_4^+$ reduces these charges. The IPP-value of the apical hydrogen drops from 1.45 to 1.28 upon ion association with Li$^+$; this value is close to that for PH$_5$. The equatorial hydrogens remain significantly charged in the presence of a cation; the IPP-values for the equatorial hydrogens are
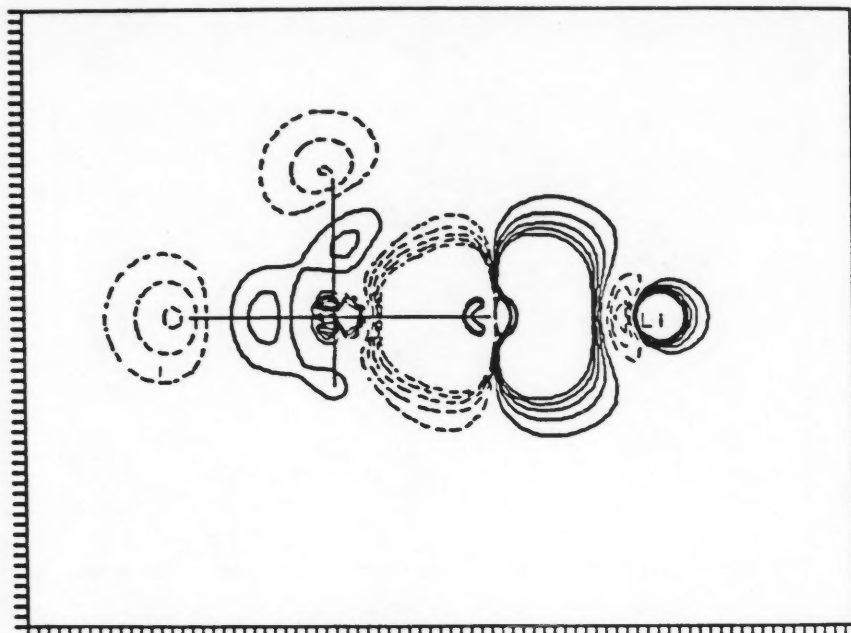
Figure 4. The 3-21G* electron density difference plot (see Figure 2 for orientation) is shown that is obtained by subtraction of the cross-sections of $PH_4O^-Li^+$ and PH_4O^-, $\rho(PH_4O^-Li^+) - \rho(PH_4O^-)$ with contour levels from -0.01 to 0.01 by 0.002 e a.u.$^{-3}$.

Table IV. Electron density analysis of PH_3O, PH_4O^-, and $PH_4O^- \cdot E$ ($E = Li^+, HF, NH_4^+$).

Molecule	Atom	C_{3v}-Symmetry		C_{2v}-Symmetry	
		MPD[b]	IPP[c]	MPD	IPP
PH_3O	O	0.548 (PO)	9.527		
	H	0.397 (PH)	1.102		
	P		13.168		
PH_4O^-	O	0.495 (PO)	9.657	0.485 (PO)	9.612
	H_a	0.317 (PH_a)	1.450	0.354 (PH_a)	1.394
	H_e	0.374 (PH_e)	1.442		
	P		12.568		
$PH_4O^-Li^+$	OLi	0.436 (PO)	11.801	0.414 (PO)	11.712
	Li	0.150 (OLi)	2.094	0.144 (LiO)	2.075
	O		9.706		9.638
	H_a	0.368 (PH_a)	1.283	0.374 (PH_a)	1.317
	H_e	0.385 (PH_e)	1.412		
	P		12.680		
$PH_4O^- \cdot HF$	OHF	0.477 (PO)	19.702		
	HF	0.131 (PH)	10.061		
	O		9.641		
	H_a	0.331 (PH_a)	1.404		
	H_e	0.380 (PH_e)	1.459		
	P		12.518		
$PH_4O^- \cdot NH_4^+$	ONH_4	0.442 (PO)	19.774		
	NH_4	0.193 (OH)	10.103		
	O		9.670		
	H_a	0.363 (PH_a)	1.305		
	H_e	0.383 (PH_e)	1.437		
	P		12.610		

[a]At RHF/3-21+(O)G*.
[b]Minimum value of the projected electron density function along the bond specified in parentheses in e a.u.$^{-2}$.
[c]Integrated projection population in electrons.

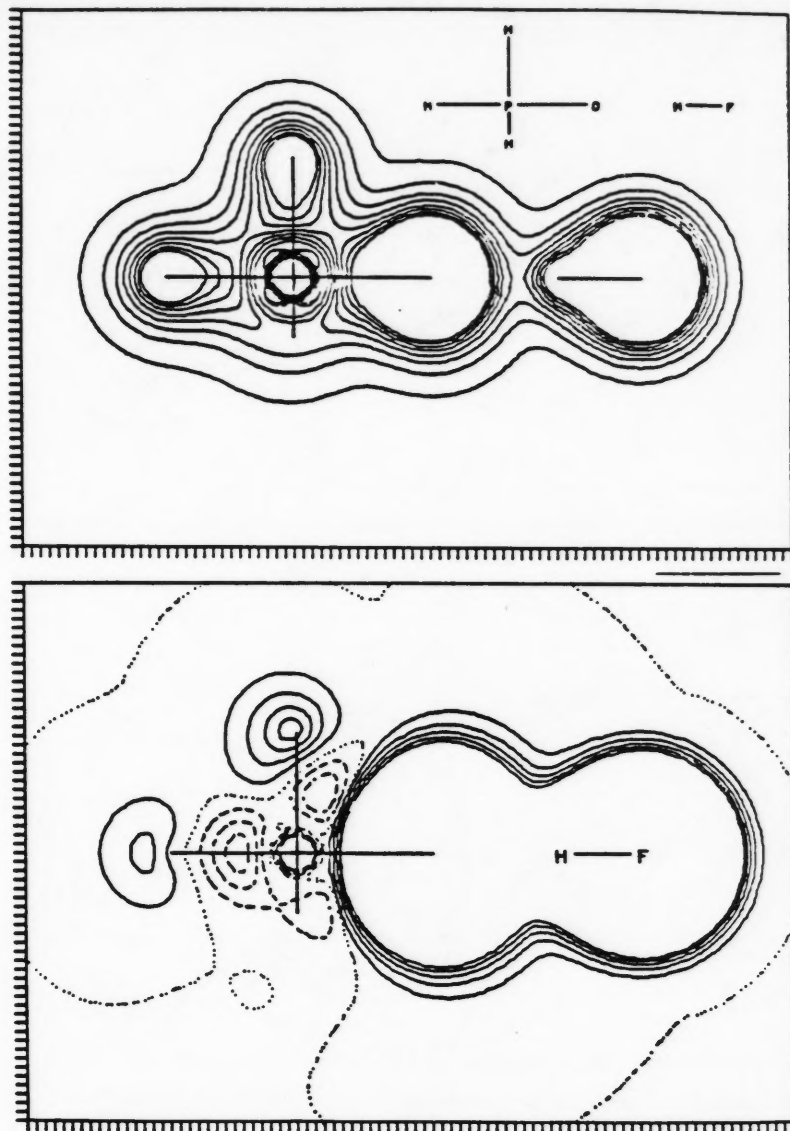**Figure 5.** On top the contour diagram is shown of the 3-21G* valence electron density cross-section of the $PH_4O^- \cdot HF$ (C_{3v}). At the bottom the difference plot is shown that results from subtraction of the cross-sections of $PH_4O^- \cdot HF$ and PH_5, $\rho(PH_4O^- \cdot HF) - \rho(PH_5)$. Contour levels are as in Figure 1.

1.41 (Li^+) and 1.44 electrons (NH_4^+) and they are closer to the respective value in PH_4O^-.

The MPD-value for the PO-bond is largest for PH_4O^- with a value of 0.50 e a.u.$^{-2}$ and close that in H_3PO (0.55). The corresponding MPD-value of the systems $PH_4O^- \cdot E$ are all lower (0.44–0.48) compared to PH_4O^-; the PO-bond strength is reduced as a result of the presence of E. The localization of electron density at oxygen in the presence of a cation is reflected in the increased IPP(O)-values compared to PH_4O^-. The HF-complexed system again behaves differently. In this case the integration of the O-population

results in a *lower* value than in PH_4O^-. This lowering is not caused by charge transfer toward HF. Charge transfer toward E is generally small and smallest in the case of the HF-complexed system. Note also that the IPP-values of the equatorial hydrogens in $PH_4O^- \cdot HF$ are larger than those in the anionic system and in $PH_4O^- \cdot E$ ($E = Li^+, NH_4^+$). The difference between the HF-complexed anion and the neutral systems appears to be caused by the different response of the σ- and π-type electron density within the PH_4O^--fragment to the presence of either a cation or HF. A cation leads to a general
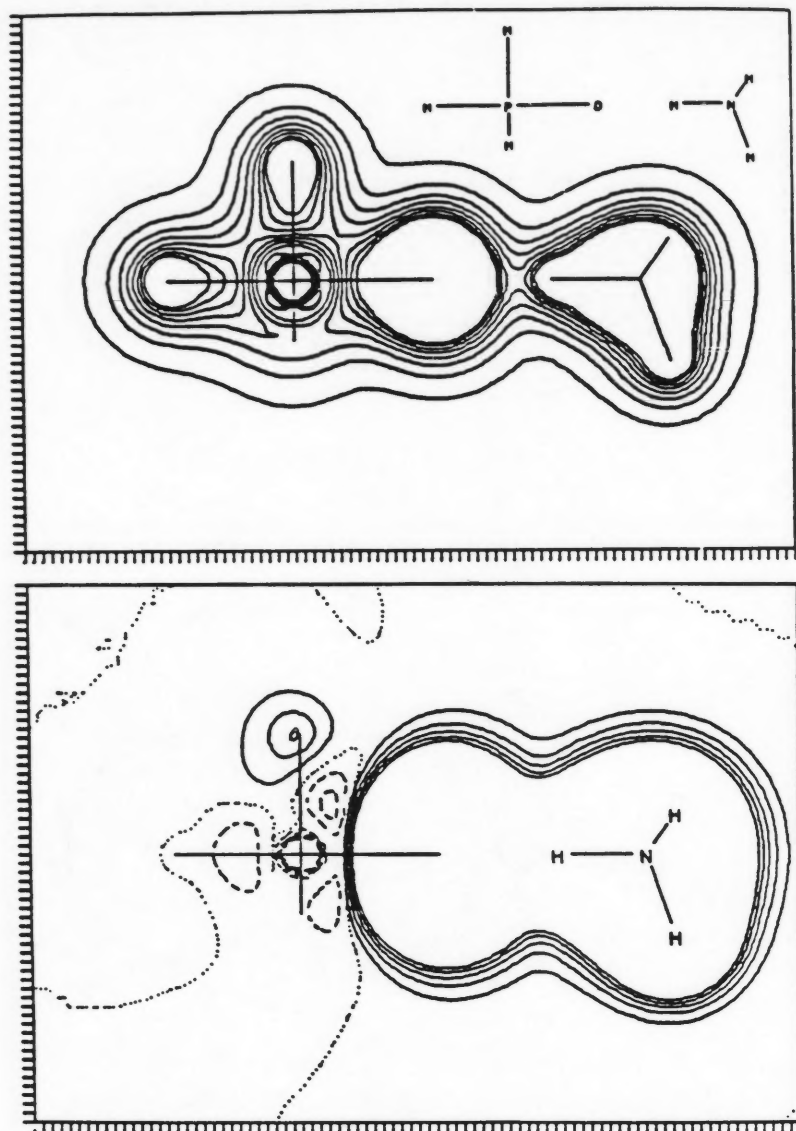
Figure 6.   On top the contour diagram is shown of the 3-21G* valence electron density cross-section of the $PH_4O^- \cdot HNH_3^+$ (C_{3v}, staggered). At the bottom the difference plot is shown that results from subtraction of the cross-sections of $PH_4O^- \cdot HNH_3^+$ and PH_5, $\rho(PH_4O^- \cdot HNH_3^+) - \rho(PH_5)$. Contour levels are as in Figure 1.

increase of the electron density at oxygen. In $PH_3O^- \cdot HF$ the H-bond localizes σ-density at oxygen. However, the repulsion between the fluorine and the π-type O-lone pairs causes an increased shift of π-electron density from oxygen to the equatorial hydrogen atoms and counteracts the increase of σ-density at oxygen. This reasoning provides an explanation for the large IPP-values of the equatorial hydrogens and is consistent with the MPD-values along the PH-bonds of $PH_4O^- \cdot HF$.

Another aspect concerns the O-populations and their relation to the charge on phosphorus. It is found that the positive charge on phosphorus *increases* as the electron population on oxygen *decreases* in all of the molecules. The π-electron donation from oxygen to the PH_4-fragment increases the electron density at the equatorial hydrogens. The overall effect of the σ-withdrawing and π-backdonating oxygen is thus essentially an increase of the polarity of the equatorial PH-bonds.
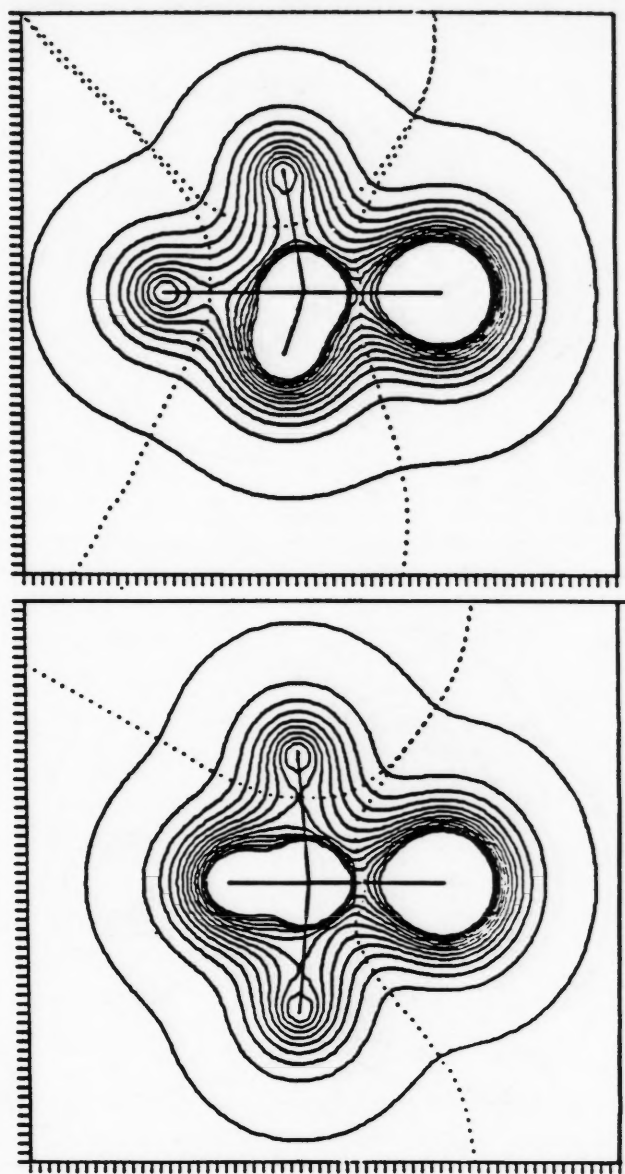
Figure 7. Contour diagrams of the 3-21G* projected electron density functions of isomeric PH_4O^- anions (C_{3v} (top) and C_{2v}; O on the right). Contour levels are from 0.005 to 0.605 by 0.05 e a.u.$^{-2}$. Demarkation lines are shown as dotted lines. See Table IV for IPP- and MPD-values.

CONCLUSION

The structures of the (di)apically substituted anions PH_4O^- and PH_3FO^- involve P-η^4-coordination and they are best described as a hydride or fluoride ion, respectively, "solvated" by phosphine oxide. Small basis sets with diffuse functions only on oxygen are inadequate, because the anionic charge is not localized on the oxygen; such basis sets probably do not allow for

an adequate functional description of the hydride or fluoride ion and they seem to result in artifactual phosphorane structures. These results suggest that computations of such structures with a potential nucleophilic leaving group in the *trans*-apical position with regard to the O⁻-substituent require in general large and/or diffuse-function augmented basis sets. This type of result may well be general for complex anions that can readily eliminate a smaller anion; the use of small
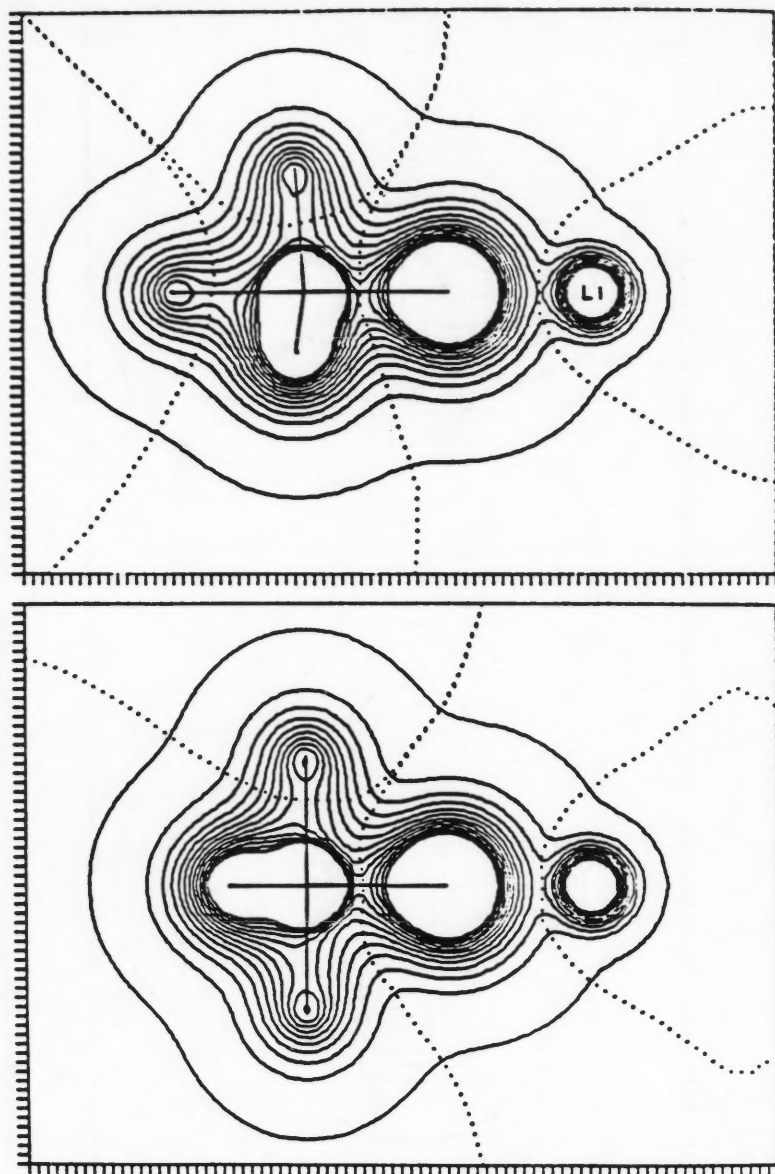
Figure 8. Contour diagrams of the 3-21G* projected electron density functions of the apically and equatorially substituted isomers of $PH_4O^-Li^+$ (C_{3v} (top) and C_{2v}; O on the right). Contour levels are as in Figure 7 and IPP- and MPD-values are listed in Table IV.

basis sets for describing such systems must clearly require due care.

Neutral derivatives of such phosphoranyloxy anions as well as derivatives in which the oxy-substituent is involved in H-bonding prefer phosphorane structures and show no or only a small tendency toward dissociation of the bond *trans*-apical to the oxy-ligand. The structures of $PH_4O_a^- \cdot E$ ($E = Li^+, HNH_3^+$), and of $PH_3FO_a^-Li^+$, as well as the model-solvated system of $PH_4O_a^- \cdot HF$ *are* phosphorane geometries

at all computational levels. These results indicate that the (Li^+O^-)-group is a suitable ligand to model phosphorus-anionic oxygen bonds in studies of multiply-substituted phosphoranes.

Molecular orbital considerations and the more rigorous results of the electron density analysis suggest that the overall neutrality of the systems causes a moderately increased localization of σ- and π-electron density at oxygen compared to PH_4O^-. Hydrogen-bonding orients the σ-type O-lone pair toward the complexing hydrogen. As
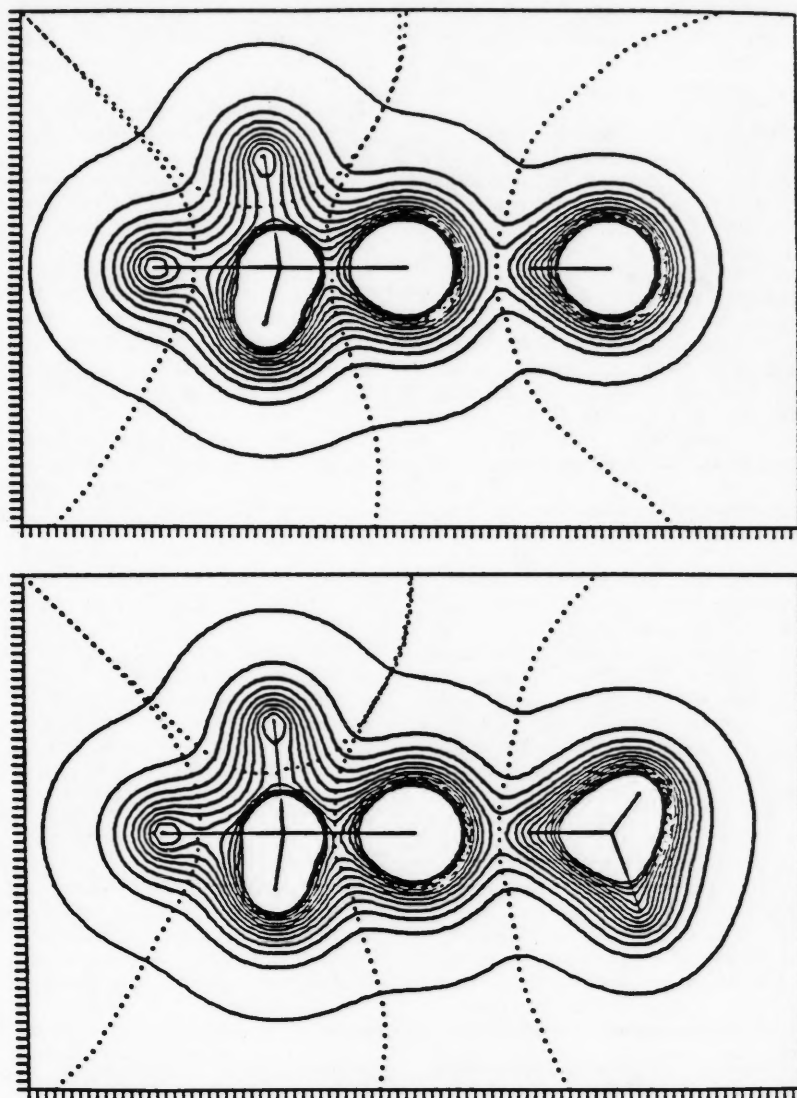
Figure 9. Contour diagrams of the 3-21G* projected electron density functions of the C$_{3v}$-symmetric model-systems PH$_4$O$^-$ · HF (top) and PH$_4$O$^-$ · NH$_4^+$ (staggered). The molecules are oriented as in Figures 5 (HF) and 6, respectively. Contour levels are as in Figure 7 and IPP- and MPD-values are given in Table IV.

a result of these polarizations the node in the σ-HOMO is shifted toward oxygen and the electron density in the bonding region between phosphorus and the *trans*-apical hydrogen is increased resulting in a stronger bond compared to the anionic oxyphosphorane.

References

1. a. R. S. McDowell and A. Streitwieser, Jr., *J. Am. Chem. Soc.*, **107**, 5849 (1985). b. At the RHF/3-21G*' level. The prime indicates a P-*d*-exponent of 0.47; see Computational Aspects.

2. See for example: a. E. J. Clementi, *J. Chem. Phys.*, **46**, 3851 (1967). b. A. Meunier, B. Levy, and G. Berthier, *Theoret. Chim. Acta.*, **29**, 49 (1973). c. A. Johansson, P. Kollman, and S. Rothenberg, *Theoret. Chim. Acta.*, **29**, 167 (1973). d. A. Pullman, H. Berthod, and N. Gresh, *Internat. J. Quantum Chem.*, **101**, 561 (1979).

3. a. Gaussian 82: J. S. Binkley, M. Frisch, K. Raghavachari, D. J. DeFrees, B. Schlegel, R. Whiteside, E. Fluder, R. Seeger, and J. A. Pople, Release A Version, Carnegie-Mellon University 1983. b. Gaussian 90, Development Version (Revision A): M. J. Frisch, M. Head-Gordon, H. B. Schlegel, K. Raghavachari, J. S. Binkley, C. Gonzalez, D. J. DeFrees, D. J. Fox, R. A. Whiteside, R. Seeger, C. F. Melius, J. Baker, R. L. Martin, L. R. Kahn, J. J. P. Stewart, E. M. Fluder, S. Topiol, and J. A. Pople, Gaussian, Inc., Pitts-

burgh PA. c. Computations with Gaussian 90 were carried out at Yale University under a license issued to Professor K. B. Wiberg. We are indebted to Professor Wiberg for the use of his computational facilities.

4. H. P. Schlegel, *J. Comp. Chem.*, **3**, 214 (1982).

5. a. J. S. Binkley, J. A. Pople, and W. J. Hehre, *J. Am. Chem. Soc.*, **102**, 939 (1980). b. M. S. Gordon, J. S. Binkley, J. A. Pople, W. J. Pietro, and W. J. Hehre, *J. Am. Chem. Soc.*, **104**, 2197 (1982). c. M. M. Francl, W. J. Pietro, W. J. Hehre, J. S. Binkley, M. S. Gordon, D. J. DeFrees, and J. A. Pople, *J. Chem. Phys.*, **104**, 5039 (1982).

6. Compare Reference 16.

7. a. W. J. Hehre, R. Ditchfield, and J. A. Pople, *J. Chem. Phys.*, **56**, 2257 (1972). b. P. C. Hariharan and J. A. Pople, *Theoret. Chim. Acta.*, **28**, 213 (1973). c. J. S. Binkley, M. S. Gordon, D. J. Defrees, and J. A. Pople, *J. Chem. Phys.*, **77**, 3654 (1982).

8. Ten mono- and six disubstituted phosphoranes have been calculated at 3-21G* and at 3-21G*. The effects on structures and relative energies are generally small except for chlorophosphorane. These results and a study of PH_4Cl will be reported separately. Structures and total energies calculated at 3-21G* and 3-21G*' for PH_5 (D_{3h}), PH_4O^- (C_{3v} and C_{2v}), and $PH_3F_aO^-$ (C_{3v} and C_s) (2 Tables) are available from the authors *via* regular or electronic mail (Bitnet: "ASTREITatUCBCMSA").

9. T. Clark, J. Chandrasekhar, G. W. Spitznagel, and P. v. R. Schleyer, *J. Comp. Chem.*, **3**, 294 (1983).

10. a. A. Streitwieser, Jr., J. B. Collins, J. M. McKelvey, D. L. Grier, J. Sender, and A. G. Toczko, *Proc. Natl. Acad. Sci. U.S.A.*, **76**, 2499 (1979). b. J. B. Collins, A. Streitwieser, Jr., and J. McKelvey, *Comput. Chem.*, **3**, 79 (1979). c. J. B. Collins, A. Streitwieser, Jr., *J. Comp. Chem.*, **1**, 81 (1980).

11. R. S. McDowell, D. L. Grier, and A. Streitwieser, Jr., *Comp. & Chem.*, **9**, 165 (1985).

12. Populations derived from the projected electron density function were originally introduced as Integrated Spatial Electron Populations, ISEP. The new nomenclature is used to prevent any confusion with the integrations over regions defined by zero-flux surfaces (Reference 14).

13. R. F. W. Baser, *Acc. Chem. Res.*, **18**, 9 (1985); and references therein.

14. R. Glaser, *J. Comp. Chem.*, **10**, 118 (1989).

15. For a review on ab initio calculations for PH_3O see: A. Streitwieser, Jr., R. S. McDowell, and R. Glaser, *J. Comp. Chem.*, **8**, 788 (1987).

16. Geometry of PH_3O (C_{3v}) in Å and degrees. a. At 3-21G*: PH = 1.393; PO = 1.460; HPO = 117.8. b. At 6-31G*: PH = 1.393; PO = 1.465; HPO = 117.0.

17. C. A. Deakyne and L. C. Allen, *J. Am. Chem. Soc.*, **98**, 4076 (1976).

18. The term *anionic oxygen* refers to oxygen in compounds with PO-bonds such as $P—O^-$, $P—O^-M^+$, and $P—O^- \cdot H—Y$ as opposed to $P—OH$ or $P—OCH_3$.

19. The study of the multiply substituted phosphoranes has been conducted in collaboration with the group of Professor P. v. R. Schleyer and the results of this study will be presented elsewhere.

20. Eigenvalues of the valence MOs of PH_4O^- and $PH_4O^-Li^+ \cdot$ $PH_4O_a^-$: $5a_1$ -1.010, $6a_1$ -0.619, $2e$ -0.378, $7a_1$ -0.306, $3e$ -0.163, $8a_1$ -0.121. $PH_4O_e^-$: $7a_1$ -1.026, $6a_1$ -0.618, $2b_1$ -0.376, $2b_2$ -0.351, $7a_1$ -0.317, $3b_2$ -0.191, $3b_1$ -0.167, $8a_1$ -0.125. PH_4O_aLi: $5a_1$ -1.206, $7a_1$ -0.812, $2e$ -0.553, $8a_1$ -0.539, $3e$ -0.372, $9a_1$ -0.317. PH_4O_eLi: $6a_1$ -1.238, $7a_1$ -0.807, $2b_1$ -0.562, $8a_1$ -0.559, $2b_2$ -0.527, $3b_2$ -0.410, $3b_1$ -0.380, $9a_1$ -0.300.

21. Standard optimized structures (Å and degrees) and total energies (atomic units). Ideal trigonal-pyramidal coordination of P and the bond lengths to hydrogen are PH_a = 1.473 Å and PH_e = 1.411 Å: PH_4O^- (C_{3v}) PO = 1.588, E = -415.796703; (C_{2v}) PO = 1.547, E = -415.818528; $PH_4O^-Li^+$ (C_{3v}) PO = 1.640, OLi = 1.621, E = -423.277757; (C_{2v}) PO = 1.577, OLi = 1.631, E = -423.279284; $PH_4O^- \cdot HF$ (C_{3v}) PO = 1.594, OH = 1.499, HF = 0.964, E = -515.347608; $PH_4O^- \cdot HNH_3^+$ (C_{3v}) PO = 1.631, OH = 1.382, HN = 1.023 (Not optimized, value as in NH_4^+ (T_d) optimized at 3-21G*), E = -472.285504; PH_3FO^- (C_{3v}) PO = 1.584, PF = 1.648, E = -514.243184; (C_s) PO = 1.518, PF = 1.648, E = -514.243184; E = -514.267317 $PH_3FO^-Li^+$ (C_{3v}) PO = 1.631, OLi = 1.617, PF = 1.620, E = -521.718844; (C_s) PO = 1.565, OLi = 1.627, PF = 1.624, E = -521.727559.

22. Comparison of the electron density difference cross-section between PH_4O^- and PH_5 (Fig. 1) with the corresponding plot[1] obtained at 3-21G*' shows that the difference in the phosphorus d-exponent has a negligible effect.

23. Calculations by D. Speer.

24. Bonds to hydrogen are associated with significantly curved zero-flux surfaces of the gradient of the electron density and the approximation of the zero-flux surface by a vertical-curtain type becomes less accurate than for other bonds.[14] The absolute value of the IPP(H)-values may therefore deviate from those resulting from density integrations employing the 3-D demarkation surface. The relative magnitudes and the changes in the IPP(H)-values should be qualitatively correct. In any case, conclusions based on the minimum projected electron density along the bonds remain valid and the arguments based on the MPD-values are consistent with the changes of the H-populations.